are equal, and J_{34} may or may not differ from J_{13} and J_{14}.

In an alternative to the simple Heisenberg description of the magnetic coupling within the cluster, expressed by Hamiltonians (A1), (A2), or (A4), a description that takes into account electron delocalization may be used. Such treatment is available for dinuclear species,[10] for the $[Fe_3S_4]^{0}$ [6-8] clusters, and for the $[Fe_4S_4]^{+}$ [9] and $[Fe_4S_4]^{3+}$ [4,26] clusters. In the case of the $[Fe_3S_4]^{0}$ clusters, it has been demonstrated that a simple Heisenberg treatment is capable of providing the same electronic description[36] as the model including electron delocalization.[5,6] This happens because there is large covariance between J values and the electron delocalization or, as generally called, the double-exchange parameter.[10] In the following, a B parameter that takes into account the tendency of the electrons to delocalize between ions at different oxidation states will be introduced according to a model previously proposed[4] and already used by us for describing the *C. vinosum* HiPIP.[26] In the presence of double exchange, Hamiltonians (A2) and (A4) are respectively transformed as[6,10]

$$\hat{\mathcal{H}} = [J(\hat{S}_1\cdot\hat{S}_2 + \hat{S}_1\cdot{}^3\hat{S}_3 + \hat{S}_1\cdot{}^3\hat{S}_4 + \hat{S}_2\cdot{}^3\hat{S}_3 + \hat{S}_2\cdot{}^3\hat{S}_4 + {}^3\hat{S}_3\cdot{}^3\hat{S}_4) + \Delta J_{12}(\hat{S}_1\cdot\hat{S}_2) + \Delta J_{34}({}^3\hat{S}_3\cdot{}^3\hat{S}_4)]\hat{O}_3 + [J(\hat{S}_1\cdot\hat{S}_2 + \hat{S}_1\cdot{}^4\hat{S}_3 + \hat{S}_1\cdot{}^4\hat{S}_4 + \hat{S}_2\cdot{}^4\hat{S}_3 + \hat{S}_2\cdot{}^4\hat{S}_4 + {}^4\hat{S}_3\cdot{}^4\hat{S}_4) + \Delta J_{12}(\hat{S}_1\cdot\hat{S}_2) + \Delta J_{34}({}^4\hat{S}_3\cdot{}^4\hat{S}_4)]\hat{O}_4 + B_{34}\hat{V}_{34}\hat{T}_{34} \quad (A6)$$

and

$$\hat{\mathcal{H}} = [J(\hat{S}_1\cdot\hat{S}_2 + \hat{S}_1\cdot{}^3\hat{S}_3 + \hat{S}_1\cdot{}^3\hat{S}_4 + \hat{S}_2\cdot{}^3\hat{S}_3 + \hat{S}_2\cdot{}^3\hat{S}_4 + {}^3\hat{S}_3\cdot{}^3\hat{S}_4) + \Delta J_{341}(\hat{S}_1\cdot{}^3\hat{S}_3 + \hat{S}_1\cdot{}^3\hat{S}_4 + {}^3\hat{S}_3\cdot{}^3\hat{S}_4) + \Delta J_{34}({}^3\hat{S}_3\cdot{}^3\hat{S}_4)]\hat{O}_3 + [J(\hat{S}_1\cdot\hat{S}_2 + \hat{S}_1\cdot{}^4\hat{S}_3 + \hat{S}_1\cdot{}^4\hat{S}_4 + \hat{S}_2\cdot{}^4\hat{S}_3 + \hat{S}_2\cdot{}^4\hat{S}_4 + {}^4\hat{S}_3\cdot{}^4\hat{S}_4) + \Delta J_{341}(\hat{S}_1\cdot{}^4\hat{S}_3 + \hat{S}_1\cdot{}^4\hat{S}_4 + {}^4\hat{S}_3\cdot{}^4\hat{S}_4) + \Delta J_{34}({}^4\hat{S}_3\cdot{}^4\hat{S}_4)]\hat{O}_4 + B_{34}\hat{V}_{34}\hat{T}_{34} \quad (A7)$$

where $\hat{O}_3$ and $\hat{O}_4$ are the occupation operators for sites 3 and 4, respectively,[6] $\hat{T}_{34}$ is the transfer operator between sites 3 and 4, and ${}^j\hat{S}_i$ (i = 3, 4; j = 3, 4) values represent the spin angular momentum operator $\hat{S}_i$ when the extra electron is on site j. B_{34} is a scalar factor proportional to the effectiveness of exchange, and $\hat{V}_{34}$ is an operator producing as eigenvalues $(S_{34} + {}^1/_2)$.[6] Such terms give the additional contributions to the energies in (A3) and (A5)

$$\pm B_{34}(S_{34} + {}^1/_2) \quad (A8)$$

In principle more than one B parameter could be used, but a report is available only for the Fe_3S_4 cluster.[8] The same order of the low-lying energy levels is obtained with and without B provided that at least one J value (the one that couples the spins connected by the transfer operator $\hat{T}_{ij}$) is properly changed. In the absence of independent information on B, the approach based only on J values is substantially equivalent to that including B.

Contribution from the Department of Medicinal Chemistry, School of Medicine, Hiroshima University, Kasumi, Minami-ku, Hiroshima 734, Japan, Coordination Chemistry Laboratories, Institute for Molecular Science, Myodaiji, Okazaki 444, Japan, and Shionogi Research Laboratories, Shionogi & Company Ltd., Fukushima-ku, Osaka 553, Japan

Synthesis, Properties, and Complexation of a New Imidazole-Pendant Macrocyclic 12-Membered Triamine Ligand

Eiichi Kimura,*[†,‡] Yasuhisa Kurogi,[†,‡] Mitsuhiko Shionoya,[†,‡] and Motoo Shiro[§]

Received May 15, 1991

A new 12-membered macrocyclic triamine with an imidazole-pendant group, 2-(4-imidazoyl)-1,5,9-triazacyclododecane (**5**), has been synthesized to study its complexation behavior with Zn^{II} and Cu^{II}, along with the ease with which the metal-bound imidazolate anion is generated. The Zn^{II} complex (**6a**) shows a close equatorial coordination of the imidazole (2.025 Å) in a distorted trigonal-bipyramidal structure with an additional chloride ion. Final R and R_w were 0.030 and 0.040, respectively: $C_{12}H_{23}N_5ZnCl(ClO_4)$, orthorhombic, space group $Pna2_1$, with a = 14.574 (1) Å, b = 9.079 (1) Å, c = 13.506 (1) Å, ρ_c = 1.627 (g cm^{-3}) for Z = 4, V = 1787.0 (3) Å^3. The proton dissociation most likely from the Zn^{II}- and Cu^{II}-coordinated imidazole (**6**, **7**) occurs with pK_a values of 10.3 and 9.3, respectively, at 25 °C and I = 0.1 (KNO_3). Mixtures of the Cu^{II} (or Zn^{II}) complex **6** and Cu^{II} (or Zn^{II}) [12]aneN$_3$ ([12]aneN$_3$ = 1,5,9-triazacyclododecane) complex **1** in alkaline CH_3OH solution yield Cu^{II},Cu^{II} (or Zn^{II},Zn^{II}) dinuclear complexes bridged by the imidazolate anion, **8**. A boron complex (**9**) has been isolated during the diborane reduction of the monooxo precursor **11**.

Introduction

Imidazole is one of the most common biofunctional ligands to play critical roles in hydrolytic nonmetallic enzymes (often "serine" enzymes) and metalloenzymes.[1] In carbonic anhydrase (CA), the Zn^{II}-bound imidazolate anion was once proposed to account for the catalytic mechanism, in which the observed proton dissociation with a pK_a value of ~7 was assigned to the imidazole (ImH) ⇌ imidazolate (Im^-) equilibrium ("zinc–imidazole" mechanism) as a result of the coordinating Zn^{II}.[2] However, the circumstantial evidence now overwhelmingly points to the H_2O ⇌ OH^- equilibrium ("zinc–hydroxide" mechanism).[3] Meanwhile, an extraneous imidazole inhibitor may replace the fourth coordinating H_2O site as an anionic Im^- ligand bonding to Zn^{II} at alkaline pH in CA.[4]

Until now, very few chemical models had been designed to test the effect of the metal coordination on ImH ⇌ Im^-. In 1976, Sargeson et al. prepared $[(NH_3)_5Co^{III}(ImH)]^{3+}$, where the $Co^{III}(ImH)$ ⇌ $Co^{III}(Im^-)$ equilibrium occurred with pK_a value of 10.0.[5] Thus, $Co^{III}(Im^-)$ had ca. 15 times higher nucleophilicity

Scheme I. Model for the CA Active Center

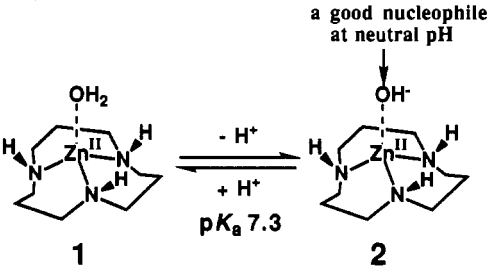

(1) Sundberg, R. J.; Martin, R. B. *Chem. Rev.* **1974**, *74*, 471.
(2) Pesando, J. M. *Biochemistry* **1975**, *14*, 675, 681.
(3) Buckingham, D. A. In *Biological Aspects of Inorganic Chemistry*; Addison, A. W., Cullen, W. R., Dolphin, D., James, B. R., Eds.; John Wily & Sons: New York, 1977; Chapter 5. Lindskog, S. In *Zinc Enzymes*; Bertini, I., Luchinat, C., Maret, W., Zeppezauer, M., Eds.; Birkhäuser: Boston, MA, 1986; Chapter 22.

[†] Hiroshima University.
[‡] Institute for Molecular Science.
[§] Shionogi and Co. Ltd.

0020-1669/91/1330-4524$02.50/0 © 1991 American Chemical Society

Scheme II

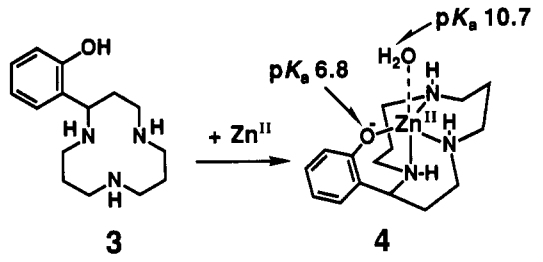

Scheme III

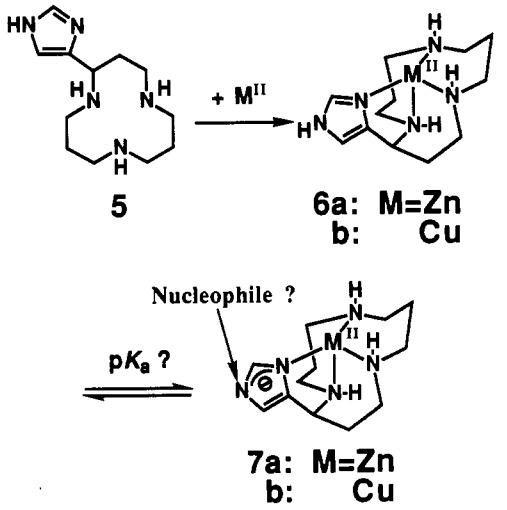

than free (noncoordinating) imidazole in the hydrolysis of *p*-nitrophenyl acetate. From this model study, the authors suspected that $Zn^{II}(Im^-)$ might be involved in the esterase activity of CA.

Very recently,[6,7] we demonstrated that a water bound to the Zn^{II} complex of a 12-membered macrocyclic triamine ([12]-aneN$_3$), **1**, has a pK_a value of 7.3 at 25 °C, which served to thermodynamically as well as kinetically support the "zinc–hydroxide" mechanism for CA (Scheme I). Meanwhile, we have reported a phenol-pendant macrocyclic triamine ligand **3** and its complex **4** with Zn^{II} (Scheme II).[8] The X-ray crystal structure of **4** has revealed a five-coordinate structure with an extremely short bonding (1.93 Å) between the phenolate oxygen and Zn^{II},[9] which (with a significantly lowered pK_a of 6.8 for the phenol and a high pK_a of 10.7 for the fifth coordinating H_2O, Scheme II) may be a suitable model to account for the phenol inhibition of CA.[10] Indeed, this complex at neutral pH showed no catalytic functions.

These results with macrocyclic triamines led us to design an imidazole-pendant macrocyclic triamine ligand **5**. In its anticipated metal complexes **6**, the imidazole nitrogen donor might come very close to the metal ions M, which would provide us with a new model to test the metal-binding effect on the imidazole deprotonation (Scheme III). A comparison of nucleophilicities of the resulting imidazolate anion in **7a** (M = Zn^{II}) and hydroxide in **2** might shed light on the role of the nucleophile in CA. Furthermore, the imidazole-pendant complex **6a** or **7a** might serve as an imidazole-inhibition model for CA.[4]

Imidazoles bound to Cu^{II} are biologically also important.[1] The present new ligand **5** might assist in better understanding the roles of imidazole coordinating to Cu^{II} ions. It was conceivable that a combination of **2** and **6** might yield a new type of imidazolate-bridging dinuclear complex **8**, which may be viewed as a

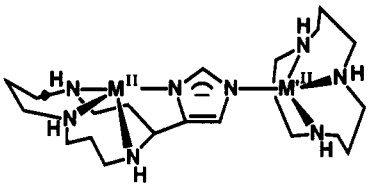

8

simplified model for Cu^{II},Zn^{II}-superoxide dismutase (SOD).[11] Earlier, several symmetrical dinuclear Cu^{II} complexes with the imidazolate bridge were reported.[12] However, until now, asymmetrical dinuclear complexes[13] or heteronuclear complexes[14] have been quite scarce.

Finally, in this work we have isolated a new boron inclusion complex **9** during synthesis of **5**. Comparison with **10**[15] is of interest with respect to the steric and/or electronic configuration of the boron.

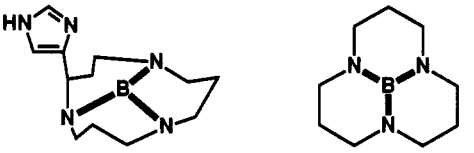

9 **10**

Experimental Section

General Methods. All commercial materials were used without further purification. ^{1}H (400 MHz) and ^{13}C NMR (100 MHz) spectra were recorded on a JEOL GX-400 spectrometer, and 3-(trimethylsilyl)-propionic-*2,2,3,3-d*$_4$ acid sodium salt for D_2O and tetramethylsilane (TMS) for $CDCl_3$ or DMSO-*d*$_6$ were used as internal references. IR and UV spectra were recorded on a Shimadzu FTIR-4200 and a Hitachi U-3200 spectrophotometer, respectively. ESR spectra, both at 25 °C and 77 K, were recorded on a JES-FE1X spectrometer using Mn^{II}-doped MgO powder as reference (g_3 = 2.034, g_4 = 1.981). Electrochemical measurements were carried out with a Yanaco P-1100 polarographic analyzer and a three-electrode cell. A saturated calomel electrode (SCE) served as the reference electrode. Melting points were determined by using a Yanaco micro melting apparatus without any corrections. Ion-exchange and thin-layer chromatographies were carried out on Amberlite IRA-400 and Merck Art. 5554 TLC plates (silica gel 60 F_{254}), respectively. Silica gel column chromatography was performed on a Wakogel C-300.

Synthesis of 4-[4-(*N*-(Triphenylmethyl)imidazolyl)]-1,5,9-triazacyclododecan-2-one (11). 3-[4-(*N*-(Triphenylmethyl)imidazolyl)]acrylic acid methyl ester (18.1 g, 46 mmol), prepared from urocanic acid (Tokyo Kasei Co. Ltd.), and 1,7-diamino-4-azaheptane (6.0 g, 46 mmol) were heated at reflux in CH_3OH/tetrahydrofuran (THF) (10:1, 900 mL) for 2 weeks. After evaporation of the solvent, the residue was purified by silica gel column chromatography with an eluent system of CH_2Cl_2/

(4) Kannan, K. K.; Petef, M.; Fridborg, K.; Cid-dresdner, H.; Lövgren, S. *FEBS Lett.* **1977**, *73*, 115.
(5) Harrowfield, J. M.; Norris, V.; Sargeson, A. M. *J. Am. Chem. Soc.* **1976**, *98*, 7282.
(6) Kimura, E.; Shiota, T.; Koike, T.; Shiro, M.; Kodama, M. *J. Am. Chem. Soc.* **1990**, *112*, 5805.
(7) Kimura, E.; Koike, T. *Comments Inorg. Chem.* **1991**, *11*, 285.
(8) Kimura, E.; Yamaoka, M.; Morioka, M.; Koike, T. *Inorg. Chem.* **1986**, *25*, 3883.
(9) Kimura, E.; Koike, T.; Toriumi, K. *Inorg. Chem.* **1988**, *27*, 3687.
(10) Pocker, Y.; Stone, J. T. *Biochemistry* **1968**, *7*, 2936.
(11) Klug-Roth, D.; Fridovich, I.; Rabani, J. *J. Am. Chem. Soc.* **1973**, *95*, 2786. Lawrence, G. D.; Sawyer, D. T. *Biochemistry* **1979**, *18*, 3045. Tainer, J. A.; Getzoff, E. D.; Beem, K. M.; Richardson, J. S.; Richardson, D. C. *J. Mol. Biol.* **1982**, *160*, 181. Tainer, J. A.; Getzoff, E. D.; Richardson, J. S.; Richardson, D. C. *Nature* **1983**, *306*, 284. Bertini, I.; Lanini, G.; Luchinat, C.; Messori, L.; Monnanni, R.; Scozzafava, A. *J. Am. Chem. Soc.* **1985**, *107*, 4391. Bertini, I.; Banci, L.; Piccioli, M. *Coord. Chem. Rev.* **1990**, *100*, 67.
(12) O'Young, C.-L.; Dewan, J. C.; Lilienthal, H. R.; Lippard, S. J. *J. Am. Chem. Soc.* **1978**, *100*, 7291. Haddad, M. S.; Hendrickson, D. N. *Inorg. Chem.* **1978**, *17*, 2622. Haddad, M. S.; Duesler, E. N.; Hendrickson, D. N. *Inorg. Chem.* **1979**, *18*, 141. Dewan, J. C.; Lippard, S. J. *Inorg. Chem.* **1980**, *19*, 2079. Drew, M. G. B. *J. Chem. Soc., Chem. Commun.* **1980**, 1122. Drew, M. G. B.; McCann, M.; Nelson, S. M. *J. Chem. Soc., Dalton Trans.* **1981**, 1868. Coughlin, P. K.; Martin, A. E.; Dewan, J. C.; Watanabe, E.; Bulkowski, J. E.; Lehn, J.-M.; Lippard, S. J. *Inorg. Chem.* **1984**, *23*, 1004. Salata, C. A.; Youinou, M.-T.; Burrows, C. J. *J. Am. Chem. Soc.* **1989**, *111*, 9278.
(13) Katz, R. N.; Kolks, G.; Lippard, S. J. *Inorg. Chem.* **1980**, *19*, 3845.
(14) Lu, Q.; Luo, Q. H.; Dai, A. B.; Zhou, Z. Y.; Hu, G. Z. *J. Chem. Soc., Chem. Commun.* **1990**, 1429.
(15) Richman, J. E.; Yang, N.-C.; Anderson, L. L. *J. Am. Chem. Soc.* **1980**, *102*, 5790. Bullen, G. J. *J. Chem. Soc., Dalton Trans.* **1981**, 511.

CH_3OH/28% NH_3(aq) (100:10:1), and recrystallization from CH_3CN/AcOEt afforded the cyclic amide **11** as colorless needles in 5% yield: TLC (eluent CH_2Cl_2/CH_3OH/28% NH_3(aq) (2:2:0.5)) R_f = 0.4; mp 248–250 °C dec; IR (KBr pellet) $\nu_{C=O}$ 1660 cm^{-1}; ^1H NMR ($CDCl_3$) δ 1.60–3.48 (m, 14 H, CH_2), 4.00 (m, 1 H, Im–CH), 5.8–6.4 (br, 2 H, amine NH), 6.61 (s, 1 H, C_4–H of Im), 6.89–7.36 (m, 16 H, triphenylmethyl and C_2–H of Im), 8.5–8.7 (br, 1 H, amide NH). Amine and amide protons were exchangeable upon addition of CD_3OD.

Synthesis of 2-(4-Imidazolyl)-1,5,9-triazacyclododecane (5). Carbobenzoxy chloride (CBZ-Cl; 0.86 g, 5.1 mmol) was added to a solution of the cyclic amide **11** (1.0 g, 2.0 mmol) and triethylamine (0.61 g, 6.1 mmol) in 100 mL of CH_2Cl_2. The solution was stirred for 1 h at room temperature. The CBZ-protected amide was obtained quantitatively after purification by silica gel column chromatography. Reduction of the amide was carried out in 36 mL of 1 M BH_3/THF solution (Aldrich) at 65 °C overnight. After treatment of 25% HBr/AcOH at room temperature for 2 h, addition of 50 mL of Et_2O afforded the final product **5** as 4HBr salts (colorless prisms, 1.1 g) in 75% yield: TLC (eluent CH_2Cl_2/CH_3OH/28%NH_3(aq) (2:2:1)) R_f = 0.3; mp >250 °C dec; *m/z* 237 (M^+, free); IR (KBr pellet) 3385 (s), 3099 (s), 2995 (s), 2700 (s, br), 1617 (m, $\nu_{C=N}$), 1467 (m), 1400 (m), 1192 (w), 1156 (w), 1082 (m), 1055 (m), 625 (w) cm^{-1}; ^1H NMR data summarized in Table V. Anal. Calcd (found) for $C_{12}H_{27}N_5 \cdot 4HBr \cdot 2H_2O$: C, 24.12 (24.27); H, 5.19 (5.06); N, 11.73 (11.79).

Synthesis of 2-(4-Imidazolyl)-1,5,9-triaza-13-boratricyclo[7.3.1.0]tridecane (9). The cyclic amide **11** (500 mg, 1.0 mmol) was reduced with 20 mL of 1 M BH_3/THF overnight at 65 °C, followed by treatment with 1 N aqueous HCl solution to deprotect the triphenylmethyl group. The mixture was poured into 0.1 N aqueous NaOH solution and extracted with several portions of CH_2Cl_2. The organic layers were combined and evaporated to dryness. The residue was recrystallized from CH_3CN to obtain the borane complex **9** as colorless plates in 36% yield: TLC (eluent CH_2Cl_2/CH_3OH (10:1) R_f = 0.4; mp 194.0 °C; IR (KBr pellet) 3420 (m, br), 2915 (s), 2809 (s), 1631 (m, $\nu_{C=N}$), 1512 (s, ν_{B-N}), 1471 (m), 1439 (s, ν_{B-N}), 1360 (s), 1323 (s), 1221 (s), 1082 (m), 841 (m), 775 (m), 662 (w) cm^{-1}; high-resolution MS calcd for $C_{12}H_{20}N_5B$ *m/z* 245.1335, obsd *m/z* 245.1813.

Preparation of [5-$Zn^{II}Cl$]ClO_4 (6a). A solution of **5**·4HCl (62 mg, 0.13 mmol) in 5 mL of CH_3OH was added to $Zn(ClO_4)_2 \cdot 6H_2O$ (49 mg, 0.13 mmol) in 5 mL of CH_3OH at room temperature. After 30 min, the resulting colorless precipitate was collected and then recrystallized from neutral H_2O. Colorless prisms of **6a** were obtained in ca. 50% yield: IR (KBr pellet) 3424 (s, br), 3308 (s), 3171 (s), 2910 (s), 1634 (m, $\nu_{C=N}$), 1495 (m), 1466 (m), 1439 (m), 1360 (m), 1275 (m), 1103 (vs), 907 (m), 864 (m), 804 (m), 628 (s) cm^{-1}. Anal. Calcd (found) for $[C_{12}H_{23}N_5ZnCl]ClO_4$: C, 32.93 (32.93); H, 5.30 (5.67); N, 16.00 (16.22). The X-ray crystal structure and analytical data for **6a** will be presented later.

Preparation of [5-$Cu^{II}Cl$]ClO_4 (6b). An aqueous solution of **5**·4HCl (62 mg, 0.13 mmol) was added to a solution of $Cu(ClO_4)_2 \cdot 6H_2O$ (49 mg, 0.13 mmol) in 5 mL of H_2O at room temperature. Slow evaporation under reduced pressure afforded the Cu^{II} complex **6b** as blue prisms in ca. 70% yield: IR (KBr pellet) 3426 (s, br), 3301 (s), 3187 (s), 2922 (s), 1635 (m, $\nu_{C=N}$), 1503 (m), 1470 (m), 1439 (m), 1358 (m), 1269 (m), 1100 (vs), 909 (m), 845 (m), 797 (m), 629 (s) cm^{-1}; UV–vis and ESR data summarized in Table VI. Anal. Calcd (found) for $[C_{12}H_{23}N_5CuCl]ClO_4$: C, 33.07 (33.16); H, 5.32 (5.47); N, 16.07 (16.10).

Preparation of the Zn^{II},Zn^{II} (8a) and Cu^{II},Cu^{II} (8b) Dinuclear Complexes. The Zn^{II}–[12]aneN_3 complex **1a** was prepared as previously described.[6] Addition of a LiOH·H_2O (0.1 mmol)/CH_3OH solution to a mixture of the Zn^{II} complex **6a** (0.1 mmol) and the Zn^{II}–[12]aneN_3 complex **1a** (0.1 mmol), in 5 mL of CH_3OH, afforded a colorless solution. After evaporation under reduced pressure, **8a** was obtained as colorless needles in 54% yield: IR (KBr pellet) 3436 (s, br), 3252 (s), 3108 (s), 2936 (s), 1628 (m, $\nu_{C=N}$), 1486 (m), 1380 (m), 1250 (m), 1108 (vs), 906 (m), 854 (m), 624 (s) cm^{-1}. Anal. Calcd (found) for $[C_{21}H_{43}N_8Zn_2](ClO_4)_3$: C, 30.14 (29.96); H, 5.18 (5.56); N, 13.39 (13.11).

The Cu^{II},Cu^{II} dinuclear complex **8b** was similarly prepared as dark green needles in 24% yield: IR (KBr pellet) 3448 (s, br), 3292 (s), 3188 (s), 2924 (s), 1630 (m, $\nu_{C=N}$), 1500 (m), 1464 (m), 1438 (m), 1382 (m), 1258 (m), 1104 (vs), 912 (m), 864 (m), 624 (s) cm^{-1}. Anal. Calcd (found) for $[C_{21}H_{43}N_8Cu_2](ClO_4)_3$: C, 30.28 (30.07); H, 5.20 (5.47); N, 13.45 (13.17). The ESR spectrum in DMSO at 77 K is given in the supplementary material. The preparation of Cu^{II},Zn^{II} heterodinuclear complexes, such as Cu^{II},Zn^{II}-SOD, by a similar method was unsuccessful.

Crystallographic Study. A colorless crystal of **6a** with dimensions 0.3 × 0.3 × 0.3 mm^3 was used for the data collection. The lattice parameters and intensity data were measured on a Rigaku AFC-5 diffractometer with graphite-monochromated Cu Kα radiation at room temperature. The structure was solved by the heavy-atom method and refined anisotropically by using absorption-corrected data to give R = 0.030 and R_w = 0.040 for 1575 independent observed reflections. The crystal of **6a**, $[C_{12}H_{23}N_5ZnCl](ClO_4)$, is orthorhombic, space group $Pna2_1$, with four molecules in the unit cell of dimensions a = 14.574 (1), b = 9.079 (1), and c = 13.506 (1) Å. All hydrogen atoms could be located in a difference electron density map. The ORTEP drawing and crystal data are shown in Figure 2 and Table I, respectively. Fractional coordinates and equivalent isotropic temperature factors are given in Table II. Selected bond distances and bond angles are shown in Table IV. The crystal collection parameters, atomic positional parameters with standard deviations, bond distances, and bond angles are given in the supplementary material.

Table I. Summary of Crystal Data, Intensity Collection, and Refinement

formula	$C_{12}H_{23}N_5O_4Cl_2Zn$
fw	437.6
cryst syst	orthorhombic
space group	$Pna2_1$
cryst color	colorless
a, Å	14.574 (1)
b, Å	9.079 (1)
c, Å	13.506 (1)
V, Å^3	1787.0 (3)
Z	4
ρ_c, g cm^{-3}	1.627
cryst dimens, mm	0.3 × 0.3 × 0.3
radiation (λ, Å)	Cu Kα (1.541 78)
μ, cm^{-1}	49.8
$2\theta_{max}$, deg	130
refinement	block-diagonal least-squares method
no. of measd reflcns	1591
no. of indep reflcns ($\|F_o\| > 3\sigma(F_o)$)	1575
R	0.030
R_w	0.040

Table II. Fractional Coordinates (×10^4) and Equivalent Isotropic Temperature Factors (×10^2, Å^2)

atom	x	y	z	B_{eq}[a]
Zn	8296.0 (2)	2271.1 (4)	1207.0 (0)	211 (1)
N(1)	8055 (2)	4380 (3)	353 (2)	227 (7)
C(2)	7933 (2)	3843 (3)	−672 (3)	247 (7)
C(4)	6752 (2)	1768 (4)	−186 (3)	251 (10)
N(5)	6956 (2)	1759 (3)	895 (2)	219 (7)
C(6)	6280 (2)	2624 (4)	1489 (3)	280 (11)
C(7)	6601 (3)	2871 (4)	2553 (4)	347 (13)
C(8)	7309 (3)	4097 (4)	2681 (3)	325 (10)
N(9)	8268 (2)	3608 (4)	2430 (3)	289 (9)
C(10)	8937 (3)	4875 (5)	2405 (3)	387 (13)
C(11)	8800 (2)	5978 (4)	1559 (4)	373 (12)
C(12)	8848 (2)	5366 (4)	513 (3)	310 (11)
N(13)	8932 (2)	1839 (3)	−94 (2)	247 (8)
C(14)	9529 (2)	877 (4)	−452 (3)	308 (10)
N(15)	9645 (2)	1113 (4)	−1424 (3)	349 (10)
C(16)	9102 (3)	2283 (4)	−1716 (4)	330 (12)
C(17)	8654 (2)	2727 (4)	−870 (3)	256 (10)
Cl	8883 (1)	247 (1)	2104 (1)	391 (3)
H(N1)	7640 (3)	4850 (4)	470 (4)	227
H(N5)	6960 (3)	920 (5)	1070 (4)	219
H(N9)	8420 (3)	3170 (6)	2920 (5)	289

[a] Anisotropically refined atoms are given in the form of the isotropic equivalent displacement parameter defined as $^4/_3 \sum_i \sum_j \beta_{ij} a_i a_j$.

Potentiometric Titrations. Aqueous solutions (50 mL) of the ligand (1.00×10^{-3} M) in the absence (for determination of ligand protonation constants) and in the presence of equimolar metal ion (for determination of complexation constants) were titrated with carbonate-free 0.100 M aqueous NaOH solution. pH values were read with an Orion 811 digital pH meter. The temperature was maintained at 25.00 ± 0.05 °C, and the ionic strength was adjusted to 0.10 M with KNO_3. −log [H^+] values were estimated with a correction of −0.08 pH unit to the pH meter readings.[16] All the solutions were carefully protected from air by a

(16) *Kagaku Binran*, 3rd ed.; Chemical Society of Japan: Tokyo, 1984; Vol. II.

Table III. Comparison of Protonation Constants and Complexation Constants for Cu^{II} and Zn^{II} at 25 °C and I = 0.1 (KNO_3)

	[12]aneN$_3$[a]	Im[12]aneN$_3$ (5)	PhOH[12]aneN$_3$ (3)[b]
log K_1	12.6	~13	~13
log K_2	7.6	7.54 ± 0.02	9.7 (phenol)
log K_3	2.4	5.20 ● 0.02 (Im)	7.1
log K_4		~2	~2
Cu^{II}: log K_{CuL}	12.6	17.6 ± 0.1	18.4[c]
Zn^{II}: log K_{ZnL}	8.8	11.7 ■ 0.1	12.6[c]

[a] From ref 20. [b] I = 0.1 ($NaClO_4$); from ref 8. [c] 1:1 complexation constants for the phenolate-M^{II} complexes **4**.

stream of humidified Ar. The electrode system was calibrated with pH 7.00 standard buffer solutions and checked by duplicate theoretical curves for the titration of 4.00 × 10^{-3} M HCl with a 0.100 M NaOH solution at 25 °C and I = 0.10 M (KNO_3) in low- and high-pH regions.

Results and Discussion

Ligand Synthesis. In a synthesis analogous to that for an imidazole-pendant cyclam,[17] the treatment of 3-[4-(*N*-(triphenylmethyl)imidazolyl)]acrylic acid methyl ester with 1,7-diamino-4-azaheptane (in 1:1 molar ratio) in refluxing CH_3OH/THF (10:1) for 2 weeks gave the anticipated 12-membered monooxo triamine **11**. The reaction mixture was purified by silica

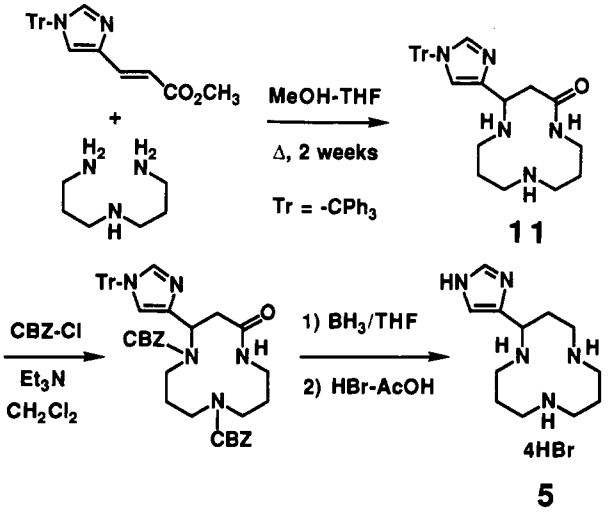

gel column chromatography with an eluent system of CH_2Cl_2/CH_3OH/28%NH_3(aq) (100:10:1), and recrystallization from CH_3CN/AcOEt afforded the product **11** as colorless needles. After the secondary amines of **11** were protected by CBZ (=carbobenzoxy) groups, the reduction of the amide function was successful with 1 M BH_3/THF, leading to the desired triamine **5** in 75% yield, isolated as crystalline 4HCl or 4HBr salts. The diborane reduction without CBZ protections for the secondary amines of **11** yielded the borane complex **9** as described later.

Protonation Constants. The experimental acid–base titration of **5**·4HBr in the absence of metal ions is shown as curve a in Figure 1. The titration data were analyzed for equilibria 1–4.

$$L + H^+ \rightleftharpoons HL^+ \qquad K_1 = [HL^+]/[L]a_{H^+} \quad (1)$$

$$HL^+ + H^+ \rightleftharpoons H_2L^{2+} \qquad K_2 = [H_2L^{2+}]/[HL^+]a_{H^+} \quad (2)$$

$$H_2L^{2+} + H^+ \rightleftharpoons H_3L^{3+} \qquad K_3 = [H_3L^{3+}]/[H_2L^{2+}]a_{H^+} \quad (3)$$

$$H_3L^{3+} + H^+ \rightleftharpoons H_4L^{4+} \qquad K_4 = [H_4L^{4+}]/[H_3L^{3+}]a_{H^+} \quad (4)$$

The log values of calculated protonation constants K_1–K_4 at 25 °C and I = 0.1 (KNO_3) are ~13, 7.54 ± 0.02, 5.20 ± 0.02, and ~2, respectively. The theoretical titration curve derived from the obtained K_1–K_4 values overlaps curves a in Figure 1. The ^1H NMR spectrum of **5** in D_2O at pD 3 showed two signals at δ 8.70 (H_a) and 7.48 ppm (H_b) assignable to the protonated imidazole

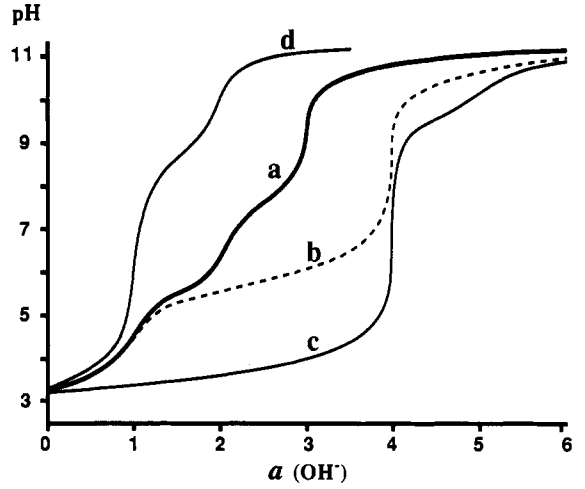

Figure 1. pH titration curves for tetraprotonated ligand **5** in the absence and the presence of equimolar Cu^{II} or Zn^{II} (I = 0.1 (KNO_3)) and monoprotonated borane complex **13** (I = 0.1 ($NaClO_4$)) at 25 °C: (a) 1.00 mM **5**·4H^+; (b) solution a + 1.00 mM $Zn^{II}SO_4$; (c) solution a + 1.00 mM $Cu^{II}SO_4$; (d) 1.00 mM **9**·H^+.

ring protons. Reversible protonation with a pK_a value of 5.2 occurs at the imidazole imide N, as evidenced by the dramatic higher field shifts of the imidazole ring protons to δ 7.45 (H_a) and 6.87 ppm (H_b) at pD 7. The proximity of the imidazole N to the 2H^+-protonated macrocycle illustrates a low pK_a value of 5.2 (normally ~7).[1]

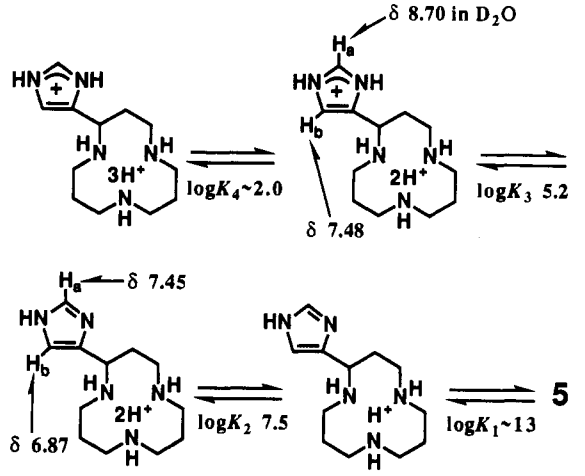

Determination of Zn^{II} and Cu^{II} Complexation Constants, K_{ML}. The titration data for **5**·4HBr in the presence of each metal ion (see curve b for Zn^{II} and curve c for Cu^{II} in Figure 1) were treated by the Schwarzenbach method[18] for the 1:1 complexes (eq 5). The metal hydrolysis (eq 6) was taken into account, where K_{OH} values are 4.6 × 10^6 for Cu^{II} and 1.1 × 10^5 for Zn^{II}.[19]

$$H_nL^{n+} + M^{n+} \rightleftharpoons ML + nH^+ \quad (5)$$

$$M^{n+} + OH^- \rightleftharpoons [M^{n+}(OH^-)] \qquad K_{OH} = [M^{n+}(OH^-)]/[M^{n+}]a_{OH^-} \quad (6)$$

The obtained 1:1 complexation constants (log K_{ML}) at 25 °C and I = 0.1 M (KNO_3) are summarized in Table III, along with those for the pendantless [12]aneN$_3$[20] and phenol-pendant [12]aneN$_3$.[8] The Cu^{II} and Zn^{II} complexes of imidazole-pendant [12]aneN$_3$ (**6**) are more stable than the corresponding complexes of pendantless [12]aneN$_3$ (**1**) but are almost the same as those of the phenolate-pendant complexes **4**.

Determination of Deprotonation Constants (pK_a) for the Zn^{II}- and Cu^{II}-Bound Imidazoles in 6. The pK_a values 10.3 (for the Zn^{II} complex) and 9.3 (for the Cu^{II} complex), for the most likely $M^{II}(ImH) \rightleftharpoons M^{II}(Im^-)$ equilibria, were estimated by pH-metric

(17) Kimura, E.; Shionoya, M.; Mita, T.; Iitaka, Y. *J. Chem. Soc., Chem. Commun.* **1987**, 1712.
(18) Schwarzenbach, G. *Helv. Chim. Acta* **1950**, *33*, 947.
(19) Bolzen, J. A.; Aruia, A. J. *Electrochim. Acta* **1962**, *7*, 589.
(20) Zompa, L. *Inorg. Chem.* **1978**, *17*, 2531.

Table IV. Comparison of ^1H NMR Data for Imidazole-Pendant [12]aneN$_3$ Derivatives

compd	solvent	δ, ppm (splitting pattern, *J* in Hz)[a]				
		H_a	H_b	H_c	H_d	H_e
5 (ligand)	D_2O (pD 7)	7.45 (s)	6.87 (s)	3.79 (dd, 8.6, 4.5)	2.63–2.86 (m)	1.56–1.83 (m)
6a (Zn–ImH)	D_2O (pD 7)	8.05 (s)	7.25 (s)	4.24 (dd, 3.6, 2.1)	2.32–3.22 (m)	1.64–2.24 (m)
	DMSO	8.20 (s)	7.34 (s)	4.76 (m)	2.29–3.42 (m)	1.23–2.25 (m)
7a (Zn–Im$^-$)	DMSO	8.12 (s)	7.28 (s)	4.68 (d, 4.6)	1.21–3.79 (m)	
8a (Zn–Zn)	DMSO	8.15 (s)	7.31 (s)	4.78 (d, 4.8)	1.23–3.81 (m)	

[a] At 25 °C in D_2O (pD 7) or DMSO-d_6 solution. The hydrogen numbering H_a–H_e follows the structure shown below.

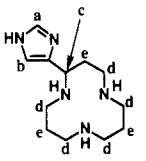

Table V. Selected Zn^{II} Bond Distances and Bond Angles in **6a**

Bond Distances, Å			
Zn–N(1)	2.263 (3)	Zn–N(5)	2.051 (3)
Zn–N(9)	2.050 (4)	Zn–N(13)	2.025 (3)
Zn–Cl	2.361 (2)		
Bond Angles, deg			
N(1)–Zn–N(5)	86.5 (1)	N(1)–Zn–N(9)	84.6 (1)
N(1)–Zn–N(13)	78.0 (1)	N(1)–Zn–Cl	167.5 (1)
N(5)–Zn–N(9)	106.3 (1)	N(5)–Zn–N(13)	102.3 (1)
N(5)–Zn–Cl	105.9 (1)	N(9)–Zn–N(13)	145.4 (1)
N(9)–Zn–Cl	93.1 (1)	N(13)–Zn–Cl	97.4 (1)

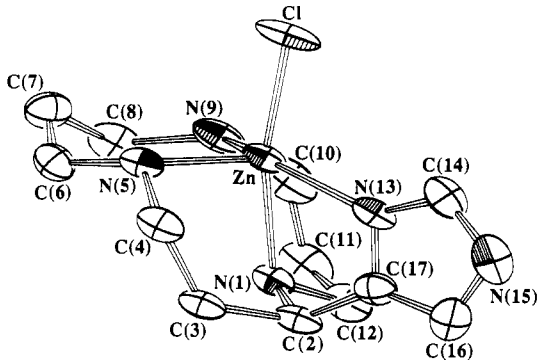

Figure 2. ORTEP diagram of [**5**–$Zn^{II}Cl$]$^+$ (**6a**), illustrating the numbering scheme. The thermal ellipsoids are drawn at the 50% level.

titrations of 1:1 ML (M = Zn^{II}, Cu^{II}) in aqueous solution at 25 °C and *I* = 0.10 M (KNO_3); see Figure 1. However, another interpretation is also likely: the base neutralization may be due to $OH_2 \rightleftharpoons OH^-$ (bound as the fifth donor, **12**).[21]

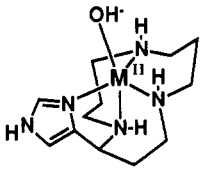

12a: M=Zn
b: Cu

We thus conducted NMR experiments to analyze the changes in the ^1H and ^{13}C chemical shifts of the imidazole ring protons and carbons of the Zn^{II} complexes **6a** and **7a**. To an aqueous solution of Zn^{II} complex **6a** were added an equimolar amount of NaOH in aqueous solution and excess sodium tetraphenylborate. The resulting colorless precipitate (analyzed as **7a**(BPh_4)) was collected and dried in vacuo. Comparison of the ^1H NMR spectra of **6a** and the isolated **7a** in DMSO-d_6 solution established that a signal of the imidazole NH proton around 13 ppm disappeared and higher field shifts occurred for the imidazole ring protons from δ 8.20 (H_a) and 7.34 ppm (H_b) for **6a** to δ 8.12 (H_a) and 7.28 ppm (H_b) for **7a** (Table IV). Furthermore, the ^{13}C NMR spectral changes for **6a** in D_2O, as pD was raised, showed that the signals of the imidazole ring carbons became broader in the pD range 10–11. We thus interpreted that the imidazolate anion (**7a**) is responsible for the longer spin–lattice relaxation (T_1) of the ring carbons.[22]

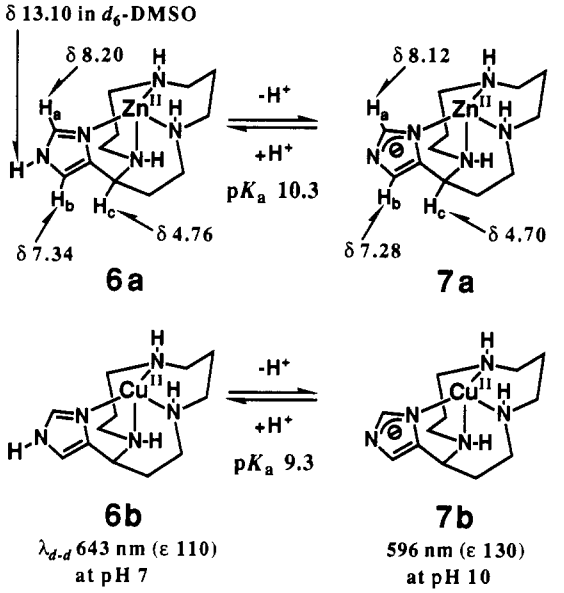

While $(NH_3)_5Co^{III}(Im^-)$ promotes the hydrolysis of *p*-nitrophenyl acetate at 25 °C in H_2O (k = 8.7 M^{-1} s^{-1}, pH 10)[5] with respect to imidazole (k = 0.6 M^{-1} s^{-1}), the $Zn^{II}(Im^-)$ complex **7a** (at pH 10–11) is practically noncatalytic.

The ImH (**6b**) $\rightleftharpoons$ Im^- (**7b**) equilibrium for the Cu^{II} complex appeared to occur as for the Zn^{II} complex. The visible absorption band for the d–d transition in aqueous solution shifted from λ_{max} 643 nm (ε 110, pH 7) to a shorter wavelength of 595 nm (ε 130, pH 10) with an increase in pH, as described for $Cu^{II}(ImH) \rightleftharpoons Cu^{II}(Im^-)$ in the literature.[23] However, this assignment is still somewhat open to question, since the formation of copper(II) hydroxide complexes also tends to cause similar shifts: λ_{d-d} 686 nm (ε 110, pH 7) for the Cu^{II}–[12]aneN$_3$ complex **1b** and 658 nm (ε 110, pH 10) for the Cu^{II}–OH^- complex **2b** in H_2O.

X-ray Crystal Structure of [5–$Zn^{II}Cl$]$^+$ (Cation of 6a). A solution of **5**·4HCl in CH_3OH was added to $Zn^{II}(ClO_4)_2 \cdot 6H_2O$ at

(21) Johnson, C. R.; Shepherd, R. E.; Marr, B.; O'Donnell, S.; Dressick, W. *J. Am. Chem. Soc.* **1980**, *102*, 6227–6235. Tweedle, M. F.; Taube, H. *Inorg. Chem.* **1982**, *21*, 3361–3371.

(22) Rahman, A. *Nuclear Magnetic Resonance*; Springer-Verlag: Tokyo, 1988.

(23) Morris, P. J.; Martin, R. B. *J. Am. Chem. Soc.* **1970**, *92*, 1543. Boggess, R. K.; Martin, R. B. *Inorg. Chem.* **1974**, *13*, 1525. Sövägo, I.; Kiss, T.; Gergely, A. *J. Chem. Soc., Dalton Trans.* **1978**, 964. Kolks, G.; Frihart, C. R.; Coughlin, P. K.; Lippard, S. J. *Inorg. Chem.* **1981**, *20*, 2933.

Chart I

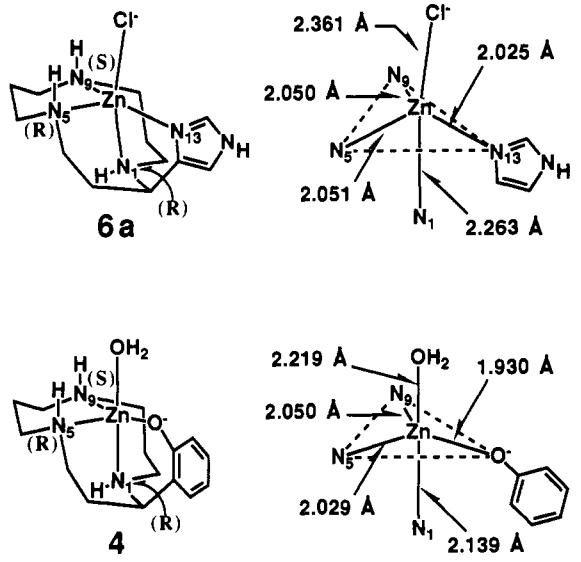

room temperature. After 30 min, the resulting colorless precipitate was collected and then recrystallized from freshly distilled H_2O. Colorless prisms of **6a** were subjected to X-ray crystal analysis. The ORTEP drawing of the cationic part of the complex (Figure 2), crystal data (Table I), and fractional coordinates and equivalent isotropic temperature factors (Table II) are provided. Selected bond distances and bond angles around Zn^{II} are given in Table V. In complex **6a**, Zn^{II} is surrounded in a distorted trigonal-bipyramidal environment by three N atoms (N_1, N_5, N_9) of the macrocyclic ligand, the imidazole nitrogen (N_{13}), and a chloride anion, as shown in Chart I.

The Zn atom lies 0.25 Å above the basal plane defined by the N(5), N(9), and N(imidazole) atoms. The apical angle N(1)–Zn–Cl is bent at 167.5°. The present five-coordinate structure may be compared with that for the phenolate-pendant [12]aneN$_3$ complex **4** (Chart I),[9] although **6a** is far more distorted than **4**. In **6a** the bond for Zn–N(imidazole) (2.025 Å) is shortest at the expense of elongated Zn^{II}–N_1, whereas in **4** the longer arm length for the phenolate O^- coordination permits a closer trigonal-bipyramidal structure with Zn^{II} remaining in a trigonal plane (formed by N_9, N_5, and O^-). The somewhat strained N_4 coordination in **6a** seems balanced sterically and electronically by the additional Cl^- coordination. The strong Zn^{II}–Im bonding explains the low pK_a value of 10.3 for ImH $\rightleftharpoons$ Im^-, almost 10^4 times lower than that for the metal-unbound imidazole. The orientations of hydrogens at the three N atoms (N_1, N_5, N_9) of the macrocycle ring in **6a** are the same as those in **4** (down, up, up or *R*, *R*, *S*),[9] which are most favorable for five-coordinate, trigonal-bipyramidal structures. On the other hand, all the NH hydrogens are "up", in the same direction as in the symmetrical tetrahedral Zn^{II} complex **2**.[6,24] Thus, we find [12]aneN$_3$ to be a suitable ligand for the Zn^{II} ion to participate in a five-coordinate, trigonal-bipyramidal or a four-coordinate, tetrahedral structure.

A distorted bipyramidal structure has been reported for the human carbonic anhydrase (CA) Zn^{II} site inhibited by an imidazole.[4] However, in view of the longer distance (~2.7 Å) between Zn^{II} and the inhibiting imidazole N, it is reasonable to assume that the dissociation of the inhibitor ImH $\rightleftharpoons$ Im^- in CA may require a higher pH than the value of 10.3 for **6a**, where Zn^{II} would exert a stronger electrophilic effect on the imidazole with the shorter distance 2.025 Å.

Borane Complex 9. The BH_3/THF reduction of **11** without the prior protection of the secondary amines by CBZ groups gave a very stable borane complex **9** in 36% yield, which is soluble in CH_3OH, CH_2Cl_2, or acidic H_2O but insoluble in neutral H_2O. **9** is so stable that attempts to hydrolyze it in 6 N HCl to recover the free ligand **5** were all unsuccessful. The B–[12]aneN$_3$ complex **10**, reported by Richman et al.,[15] has a very stable BN_3 trigonal-planar array with B taking an sp^2 hybridization, which resists any degradation methods.

Scheme IV

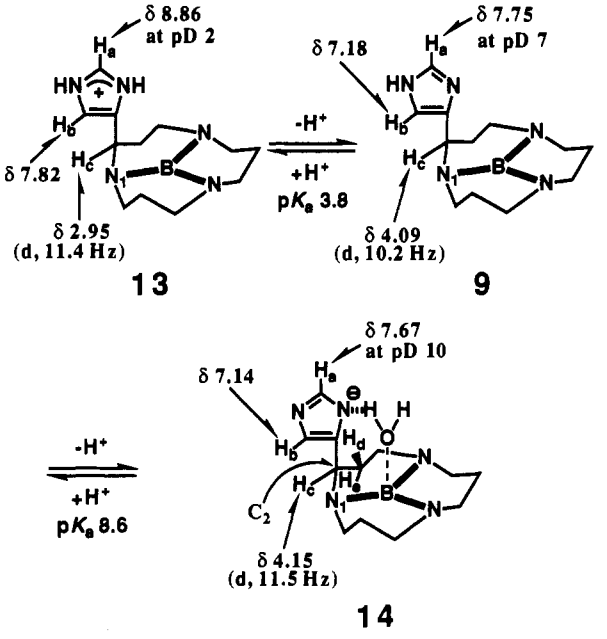

Chart II

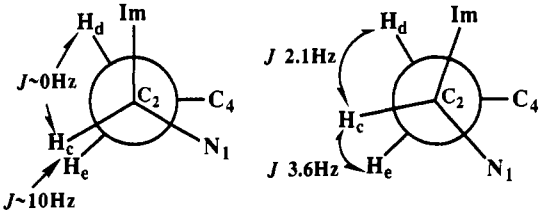

An interesting question as to whether the imidazole N binds to B might be solved by the ^{1}H NMR measurements (Scheme IV). The borane complex dissolved into pD 2 solution may be tentatively presented as **13**, where two specific ^{1}H NMR signals appear at δ 8.86 (H_a) and 7.82 (H_b) for the imidazole ring protons. The deprotonation reversibly occurs with a pK_a value of 3.8 (pH-metrically determined at 25 °C and I = 0.1 ($NaClO_4$), Figure 1d) at the imidazole N, as evidenced by the dramatic higher field shift of the imidazole protons to δ 7.75 (H_a) and 7.18 ppm (H_b) at pD 7 (Scheme IV). The titratable imidazole (with H^+) implies a weak interaction between Im and B in **9**. If the ImH–B interaction is stronger (as in the Zn^{II} and Cu^{II} complexes **6**), such protonation would not occur at pH 2.

The methyne proton (H_c) at C_2 attached to the imidazole group showed almost the same doublet pattern (J = 10–11 Hz) regardless of pH change. This suggests that one of the vicinal methylene protons (H_d) at adjacent C_3 almost eclipses H_c (J = 10–11 Hz) and the other (H_e) is almost perpendicular to H_c (J ~ 0 Hz); see the Newman projections in Chart II. Such a conformation seems possible if the imidazole group remains perpendicular to the BN_3 trigonal-planar array regardless of pH. It is thus concluded that the imidazole N remains uncoordinated to the B atom. On the other hand, in the Zn^{II} complex **6a**, the H_c proton appeared as a doublet of doublets, which suggests a somewhat staggered position with respect to H_d and H_e (Chart II). The strong Im–Zn^{II} binding should cause such a conformation.

The infrared spectrum of **9** (KBr pellet) shows characteristic B–N stretching frequencies at 1512 and 1439 cm^{-1}, suggesting strong B–N bonding with π-bond character, as found for the

(24) Schaber, P. M.; Fettinger, J. C.; Churchill, M. R.; Nalewajek, D.; Fries, K. *Inorg. Chem.* **1988**, *27*, 1641.

trigonal-coplanar **10** (ν_{B-N} 1510 and 1440 cm^{-1}).[15] The second deprotonation with a pK_a value of 8.6 was pH-metrically determined at 25 °C and I = 0.1 ($NaClO_4$) (Figure 1). On the basis of the disappearance of the imidazole NH proton in the ^1H NMR spectrum ($CDCl_3$) and the similar ν_{C-N} values of 1516 and 1447 cm^{-1}, we tentatively assign a structure **14**, where the imidazolate may be appreciably stabilized by a water associating with B.

Synthesis of Dinuclear Complexes 8. Addition of an equimolar amount of $LiOH·H_2O$ to a mixture of the Zn^{II} (or Cu^{II}) complex **6** and the Zn^{II} (or Cu^{II}) [12]aneN$_3$ complex **1**[20] in CH_3OH afforded the Zn^{II},Zn^{II} (or Cu^{II},Cu^{II}) dinuclear complex **8a** (or **8b**). However, crystalline heteronuclear Cu^{II},Zn^{II} complexes could not be isolated by mixing **6a** with **1b** or **6b** with **1a**.

The Zn^{II},Zn^{II} dinuclear complex **8a**, which is the first example of this type, was obtained as colorless needles in 54% yield.

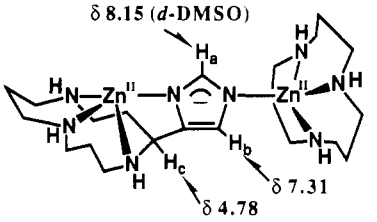

8a

Though stable in anhydrous CH_3OH, **8a** is very sensitive to H_2O. **8a** immediately dissociates, upon contact with H_2O, to the component complexes **6a** and **2a**. In addition to the elemental analysis, supporting evidence for the **8a** structure was obtained from comparison of the ^1H NMR patterns (DMSO-d_6) for **6a**, **7a**, and **8a** (Table IV). Comparison of the ^1H NMR spectra of **6a** and the isolated **8a** in DMSO-d_6 established that the imidazole NH proton signal around 13 ppm disappeared, accompanied by the higher field shifts of imidazole ring protons from δ 8.20 (H_a) and 7.34 ppm (H_b) for **6a** to δ 8.15 (H_a) and 7.31 ppm (H_b) for **8a** as well as **7a** (δ 8.12 (H_a) and 7.28 ppm (H_b)). However, crystals suitable for X-ray study were not obtained, and hence more detailed characterization could not be made.

The Cu^{II},Cu^{II} dinuclear complex **8b** was similarly isolated as dark green needles in 24% yield. In addition to the elemental analysis, supporting evidence for a Cu^{II}–Cu^{II} spin coupling through

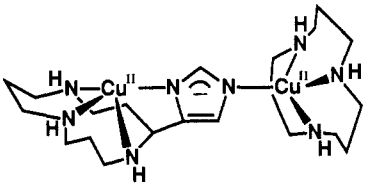

λ_{d-d} 668 nm (ε 390) in CH_3OH

8b

the bridging imidazolate in **8b** was obtained from an ESR spectrum at 77 K in DMSO glass (0.1 M Et_4NClO_4), which showed a weak $\Delta M = \pm 2$ transition at half-field (~1560 G, Table VI). The $\Delta M = \pm 2$ transition similarly occurs at ~1520 G in an analogue[12] and at ~1540 G in Cu^{II},Cu^{II}-SOD.[25] The $A_\parallel$ value of 98 G for **8b** indicates a tetrahedral coordination such as in Cu^{II},Cu^{II}-SOD, which is different from other square-planar SOD-model complexes ($A_\parallel$ ~ 180 G).

The visible absorption (d–d transition, Table VI) of the Cu^{II},Cu^{II} dinuclear complex **8b** (668 nm, ε 390) in anhydrous CH_3OH is different from those of the mixture of the mononuclear Cu^{II}–imidazole complex **6b** (629 nm, ε 220) and Cu^{II}–[12]aneN$_3$ complex **1b** (650 nm, ε 210). The visible absorptions of previously studied N_3Cu^{II}–Im–$Cu^{II}N_3$ dinuclear complexes all occurred at ~620 nm with square-planar ligand fields.[12] A strong shoulder, at ~360 nm, for **8b** is common to the imidazolate-bridged complexes Cu^{II},Zn^{II}- and Cu^{II},Cu^{II}-SOD (both at ~450 nm);[25] however, in previous studies of Cu^{II},Cu^{II} dinuclear complexes this characteristic was not reported. We conclude that this shoulder is due to the Cu^{II}–Im–Cu^{II} transition. The polarogram of **8b** in DMF (at 25 °C and I = 0.2 (Et_4NClO_4)) showed an irreversible reduction wave for $Cu^{II} \rightarrow Cu^0$, which differs from the irreversible $Cu^{II} \rightarrow Cu^0$ wave of **6b**.

Table VI. Comparison of UV–Vis and ESR Data for Cu^{II} Complexes

		ESR (77 K)[b]			
compd	UV–vis:[a] λ_{max}, nm (ε)	$g_\parallel$	$g_\perp$	$A_\parallel$, G	$\Delta M = \pm 2$, G
1b	275 (2900), 650 (210)	2.24	2.05	169	
6b	291 (6300), 629 (220)	2.21	2.05	158	
7b	265 (8400), 608 (210)	2.21	2.05	155	
8b	253 (8200), ~360 (sh, ~1800), 668 (390)	2.10	2.08	98	~1560
SOD[c]	~450 (sh), 800	2.27	2.07	146	~1540

[a] At 25 °C in CH_3OH; ε in M^{-1} cm^{-1}. [b] In DMSO (I = 0.1 M (Et_4NClO_4)). [c] Cu^{II},Cu^{II}-SOD in H_2O (pH 7.8); from ref 25.

Judging from the disapperance of the $\Delta M = \pm 2$ transition peak (ESR) and of the shoulder at ~360 nm (UV–vis), **8b** was easily decomposed to **6b** and **2b** upon contact with H_2O, probably because of the unstable tetrahedral coordination around Cu^{II}. In contrast, the square-planar Cu^{II},Cu^{II} dinuclear complexes are more stable in neutral H_2O.

In an attempt to prepare the more interesting Cu^{II},Zn^{II} heterodinuclear complexes, **6a** (or **6b**) was mixed with **1b** (or **1a**) in CH_3OH with an equimolar amount of CH_3ONa. In both cases, the UV–vis spectra of the reaction mixture showed absorption bands similar to those of the mononuclear Cu^{II} complex **7b** but no absorption around ~360 nm suggestive of imidazolate-bridged metal ions. The polarogram of the reaction mixture in DMF (at 25 °C and I = 0.2 (Et_4NClO_4)) also showed a $Cu^{II} \rightarrow Cu^0$ reduction wave similar to that of **7b**. From this evidence, it is clear that we were unable to prepare the Cu^{II},Zn^{II} dinuclear complexes from **6** and **1**.

Conclusion

The newly synthesized compound imidazole-pendant [12]aneN$_3$ (**5**) is the first ligand to be used in the preparation of a five-coordinate, trigonal-bipyramidal Zn^{II} complex containing a short intramolecular Zn^{II}–ImH bond. Despite the fact that the Zn^{II}–ImH bond is indeed strong, with a distance of 2.025 Å in the 1:1 complex **6a**, the Zn^{II}(ImH) ⇌ Zn^{II}(Im^-) equilibrium occurs with a pK_a value of 10.3 (at 25 °C and I = 0.1 (KNO_3)) but not with a value as low as 7.3, which was found for the Zn^{II}-bound H_2O in **1**. We have shown that Zn^{II}(Im^-) does not function catalytically in the hydrolysis of esters. Zn^{II},Zn^{II} (**8a**) and Cu^{II},Cu^{II} homodinuclear complexes (**8b**) containing an imidazolate bridge were isolated by mixing **1** and **6** in alkaline CH_3OH solution. However, they are very unstable and dissociate readily in H_2O. Attempts to prepare Cu^{II},Zn^{II} heterodinuclear complexes similar to the Cu^{II},Zn^{II}-SOD model have failed, due to the more facile reverse dissociation process.

Acknowledgment. We thank the Japan Shipbuilding Industry Foundation and the Shimadzu Science Foundation for Scientific Research Grants.

Registry No. **1a**, 128217-16-3; **1b**, 136823-74-0; **5**, 136838-30-7; **5**·4HBr·2H_2O, 136823-64-8; **5**·4HCl, 136823-65-9; **6a**, 136823-69-3; **6b**, 136823-71-7; **7a**(BPh_4), 136823-76-2; **7b**, 136823-77-3; **8a**, 136838-32-9; **8b**, 136823-73-9; **9**, 136823-66-0; **11**, 136823-67-1; $H_2NCH_2CH_2NHCH_2CH_2NH_2$, 56-18-8; BH_3, 13283-31-3; 3-[4-(*N*-triphenylmethyl)-imidazolyl)]acrylic acid methyl ester, 112606-55-0.

Supplementary Material Available: Tables of atomic positional parameters, bond distances, and bond angles and the ESR spectrum of **8b** in DMSO solution (5 pages); a listing of observed and calculated structure factors (11 pages). Ordering information is given on any current masthead page.

(25) Fee, J. A.; Phillips, W. D. *Biochim. Biophys. Acta* **1975**, *412*, 26. Valentine, J. S.; Pantoliano, M. W.; McDonnell, P. J.; Burger, A. R.; Lippard, S. J. *Proc. Natl. Acad. Sci. U.S.A.* **1979**, *76*, 4245.